Innovative: International Multi-disciplinary Journal of Applied Technology
(ISSN 2995-486X) VOLUME 03 ISSUE 12, 2025

Hydraulic Modeling of Vane Pump Parameters

B.Khamdamov
Doctor of Technical Sciences, Associate Professor of the Department of Tashkent State Technical University named after I.A. Karimov.
*Email:*_khamdamov_55@mail.ru

R.K.Dusmatov
Ph.D., Associate Professor of the Department of Tashkent State Technical University named after I.A. Karimov.
Email: iis_ravshan@mail.ru

A.B.Saparov
Regional Coordinator of the Asian Development Bank, Nukus, Uzbekistan.
Email: Aza-saparov@mail.ru

N.R.Nasyrova
Doctoral student. Scientific Research Institute of Irrigation and Water Problems, Tashkent, Uzbekistan.
Email: n_naira1982@mail.ru

G.S.Azizova
Doctoral student of the Department of Tashkent State Technical University named after I.A. Karimov.
*Email:*azizovagulnoza764@gmail.com

Abstract:

An analysis of previous studies shows that performance optimization issues in three-dimensional impellers of vane pumps have been insufficiently explored. In a meridional plane, the vanes rotate from an axial to a radial direction in three dimensions. However, the flow studies are primarily limited to those near the impeller inlet and outlet. The goal of these studies is to improve the pump flow path to reduce impeller cavitation wear and improve operating parameters. The data obtained in the study were statistically processed, and based on them, pump design options with optimal parameters can be developed. The article presents key recommendations for studying

transient processes using OPV and V-type pump units with an impeller diameter of D_r = 250 mm. The influence of cavitation on the pressure pulsation pattern was determined. Software studies were used to determine the compatibility of impeller modes, which are designed using formulas for high- and low-pressure zones, thereby increasing pump efficiency by 3-5%.

Keywords: pumping units, optimal parameters, pressure, flow path, impeller, blade, cavitation.

Introduction

In practice, there are cases of prolonged operation of pumps with greatly increased hydraulic losses in the suction line with low water levels in the downstream pool and mechanical damage to pump components due to cavitation. Experience in operating pumping stations has necessitated the justification and experimental verification of the efficiency of pumps [1,2].

In laboratory experiments, the solution conditions are free vibrations of the model, where the boundary conditions are unconstrained and unloaded. After calculations, it was found that the first natural frequencies of the vane pump are practically zero. This is due to the model's structural and dynamic stability. Initial signs of instability are visually detected by erosion, vibration, and noise from the impeller and the pump as a whole when cavitation occurs.

Cavitation significantly reduces the efficiency of pumping equipment, but early detection of cavitation effects allows for maintaining its functionality, extending its service life, and taking measures to prevent further damage. Even at very low levels, cavitation can be detected using specialized instruments [3,4].

Main body.

The hydrodynamic properties of vane pumps are largely determined by the direction and magnitude of the fluid flow velocity. The boundaries of the fluid flow in the pump are the walls of the flow path, which consists of the inlet and outlet of the impeller [1,2].

The movement of fluid in the interblade channels of an impeller is complex. The velocity triangles at the impeller inlet change sharply with flow eddies at the blade inlet and with direct inlet (Fig.1).

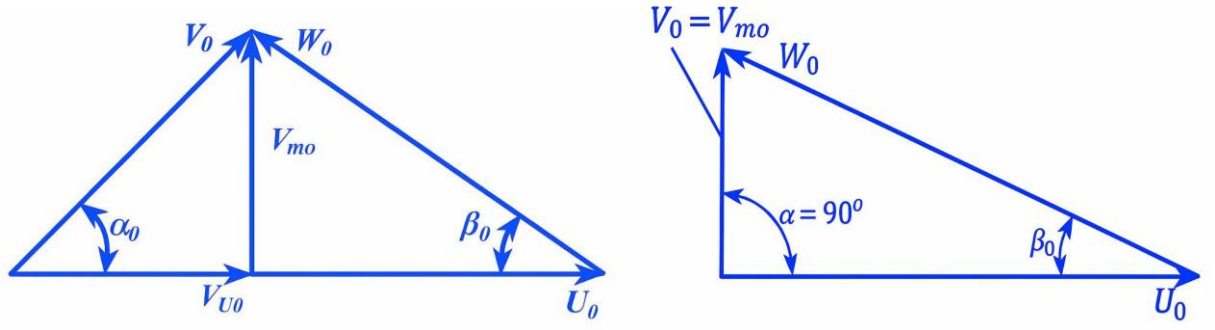

a) b)

a – vortex conditions; b – direct entry

Fig. 1. Conditions for velocity entry into the impeller

Let us introduce the following notations: α is the angle between the absolute V and the transfer U velocities of the fluid; β is the angle between the relative velocity W and the negative direction of the transfer U velocity of the fluid. Further, the subscript "0" is used for the flow at the impeller inlet.

The relative velocity W_0 of the flow in front of the blades is found from the triangle. The direction of the velocity Wo is determined by the angle β_0 to the transfer velocity U_0. After the flow enters the blades, two motions are considered: one reflecting only the flow restriction by the blades and the other characterizing the total impact of the blade on the flow.

The restriction of the flow by the blades does not change the angular momentum of the fluid and, therefore, cannot affect the magnitude of the circumferential component of the absolute velocity. The generalization of the performance indicators and main geometric parameters of the manufactured pumps is carried out on the basis of a theory where the similarity criterion is the pump speed coefficient.

$$n_s = \frac{3{,}65 \cdot n \cdot \sqrt{Q}}{H^{3/4}}, \quad (1)$$

Where H is the pump head, m;

Q is the pump flow rate, m^3/s;

n is the impeller speed, min^{-1}.

Determining the values of the coefficient ns determines the design of the liquid supply to the impeller (Fig. 2).

a b c d

Fig. 2. Fluid supply diagrams (a) to the impeller inlet (b, c) with a sealing ring (d)

If n_s<40, the pump should be multistage with sequential impellers. The total pump head should be distributed among the stages as $H = H_{r1} + \ldots H_{ri}$.

The choice of blade angle at the outlet, β, is determined by the speed coefficient and the required shape of the pump's pressure characteristic. Based on operating experience, the table shows average values for the pumps tested.

Table - Range of n_s variation

n_s	β
50…100	35°…30°
100…200	25°…20°
250…400	21°…17°

In certain cases where high pressure is required, the β angle can be selected to be up to 40°. This increases the diffuser area of the interblade channel, which reduces the impeller's efficiency. The use of larger β angles is also limited by increased losses in the outlet diffuser devices.

The analytical method for calculating the blade of a centrifugal pump wheel provides a mathematical description of the blade's centerline, which makes it possible to smoothly outline it, taking into account the accepted blade installation angles at the inlet and outlet.

Experience in operating centrifugal pumps shows that wear of the inlet parts of the blades is predominant (Fig. 3).

Fig. 3. Wear of the inlet parts of the blades

The leading edge of the blades exhibits four distinct areas with varying degrees and patterns of wear. Medium to severe wear, visible as flakes, is observed at the leading edge (vertical section). The horizontal section of the leading edge is damaged by deep, slit-like grooves reaching 25 mm in depth. The adjacent strip (200-250 mm wide) is marked by deep striated wear. The grooves are oriented at an angle to the vertical portion of the blade and fan out toward the bottom. The trailing edges on the curved sections are severely damaged and jagged. Metal tears reach a depth of 200 mm across the blade's width, and their total area can be up to 300 cm².

The impeller wear curve along the outer diameter increases parabolically up to 100 hours of pump operation (Fig. 4). After that, it changes linearly.

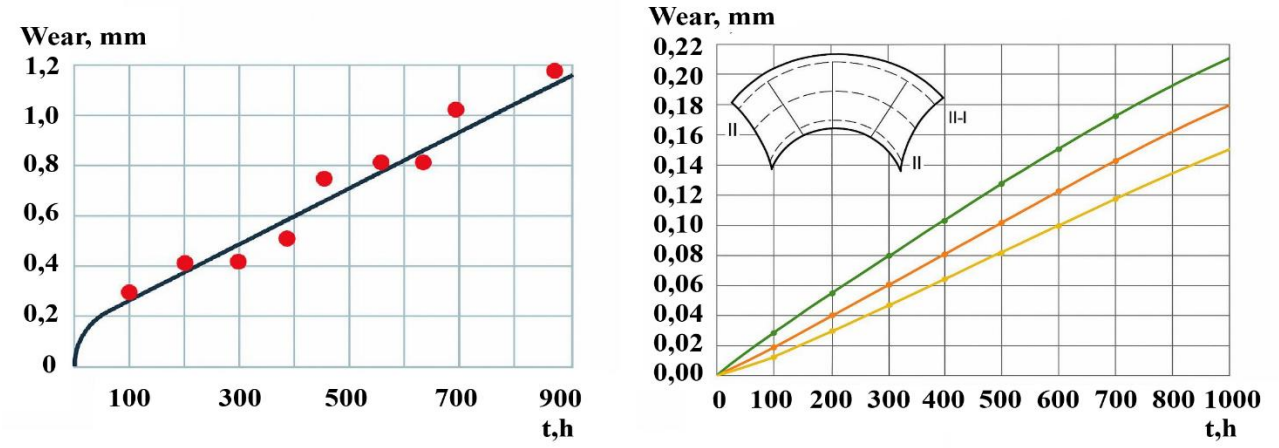

a) b)

a) - cavitation-abrasive wear; b) - abrasive wear

Fig. 4 - Dynamics of impeller wear along the outer diameter D.

This can be explained by the fact that up to 100 hours of pump operation, abrasive particles have a more intense effect on wear, since the gap between the impeller and the chamber is still small, and on the other hand, during this period the concentration of solid particles in the pumped water is usually the highest. With continued operation of the pump, wear of the impeller increases uniformly.

When clarifying the influence of hydrothermodynamics on the cavitation characteristics of a pump, it was established that one of the main parameters determining the suction capacity of a pump, and consequently its cavitation characteristics, is the value of H^{sv} or excess suction head. These values can be improved by switching to impeller shapes that increase their service life by 2 times.

The question of how to convert model experiment data to real-world data is a key one when studying non-stationary processes in pump flow paths.

The operating principle of a vane pump is shown in Fig. 5.

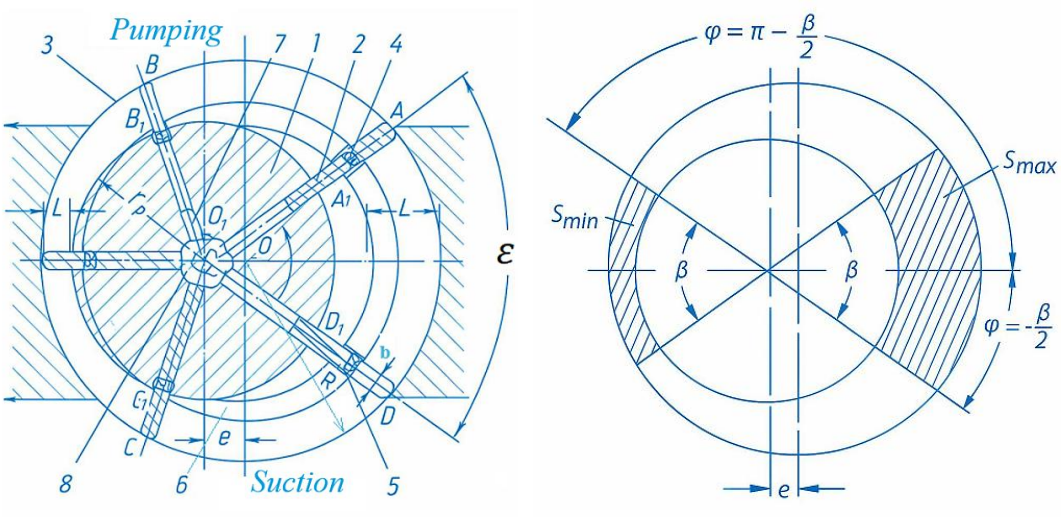

a) b)

1-rotor; 2-blades; 3-stator; 4-axles; 5-sealing rings; 6-grooves; 7-chambers; 8-channels
Fig. 5. The operating principle of the pump and the calculation of the maximum S_{max} and minimum S_{min} areas of the chambers formed between the blades.

By expanding the area of CDD_1C_1, conditions arise for improving the absorption of liquid from the supply to the wheel. A special sealing barrier is used to ensure a tight seal and isolate the discharge line from the suction line.

To describe the blade centerline using the Archimedean spiral equation, the following equation is analyzed $\rho = R + \alpha\varphi$, where α is the pitch of the spiral, R is the stator radius.

To increase efficiency, forced-action blades can be used. The blade ends are equipped with axles (4) and special sealing rings (5) that fit tightly to the housing and impeller, reducing fluid leakage. This allows the blades to actively participate in fluid transfer, increasing pump performance.

The main dependencies of the described elements are designed according to the formulas:

$$l = R - r_r - l; \tag{2}$$

$$L = R - r_r + l, \tag{3}$$

The difference between the lengths and the radius of the rotor L and l, r_r determines the blade stroke

$$L - l = 2e. \tag{4}$$

The value e in Fig. 5 for pumps with adjustable capacity is variable. If $e = 0$, then based on equations (2) and (3)

$$L = l = R - r_r. \tag{5}$$

If $e = e_{\max}$, then $R - r_r = e_{max} + l_{min}$ and $L = 2e_{\max} + l_{\min}$.

The largest value of the area of the chamber between the blades will be determined if we take $\varphi = -\frac{\beta}{2}$ (Fig. 1b)

$$S_{\max} = \frac{e^2}{2} \cdot \sin\beta + R \cdot e \sin\frac{\beta}{2}\sqrt{1-(\frac{e}{R}\sin\frac{\beta}{2})^2} + R^2\, arcsin\frac{e}{R} sin\frac{\beta}{2} + \frac{R^2-r_r^2-e^2}{2}\beta. \quad (6)$$

The smallest value of the area of the chamber between the blades will be determined if we take $\varphi = \pi - \frac{\beta}{2}$.

$$S_{\min} = \frac{e^2}{2}\sin\beta - R \cdot e \sin\frac{\beta}{2}\sqrt{1-(\frac{e}{R}\sin\frac{\beta}{2})^2} - R^2 \cdot arcsin\frac{e}{R} sin\frac{\beta}{2} + \frac{R^2-r_r^2-e^2}{2}\beta. \quad (7)$$

Pump capacity

$$Q = (S_{\max} - S_{\min})B \cdot n \cdot z, \quad (8)$$

Подставляя в последнее уравнение значения S_{max} и S_{min}, определяемые уравнениями (6) и (7), получим

where B is the rotor width, m;

n is the rotor speed, rpm.

Substituting into the last equation the values of S_{max} and S_{min}, determined by equations (6) and (7), we obtain

$$Q = 2 \cdot R\left[e \cdot \sin\frac{\beta}{2}\sqrt{1-(\frac{e}{R}\sin\frac{\beta}{2})^2} + R\arcsin\frac{e}{R}\sin\frac{\beta}{2}\right]B \cdot n \cdot z. \quad (9)$$

Given that, usually, $\frac{e}{R} \le 0{,}1$ one can accept without significant error $\sqrt{1-(\frac{e}{R}\sin\frac{\beta}{2})^2} \cong 1$; $\arcsin\frac{e}{R} \cong \frac{e}{R}$.

Then

$$Q = 4R \cdot e \cdot B \cdot n \cdot z \sin\frac{\beta}{2}. \quad (10)$$

Calculation of values using formulas (6) – (10) determines the hydraulic suction conditions for the operating parameters.

Conclusion:

1. The results of transferring a model experiment to a real one were studied for non-stationary processes in the flow path of pumps that reduce liquid leakage. Calculations were performed and key relationships were established, which formed the basis for the design of pump components. The use of formulas for high- and low-pressure zones allowed for an increase in overall pump efficiency.

2. The work utilized the fundamental principles of vane pump theory, and the similarity criterion was the pump speed coefficient. For vane pumps, the total pump head is distributed among the impeller

stages. The choice of the blade angle at the outlet is determined by the speed coefficient and the shape of the pump pressure characteristic.

3. Experiments determined the effect of pressure on the pressure pulsation amplitude. When clarifying the influence of hydrothermodynamics on the pump's cavitation characteristics, it was established that the values of excess pressure and geometric suction lift are among the key parameters.

References:

1. Yu. D. Zemenkov et al. Operation of pumping and power equipment at pipeline transport facilities // Tyumen, 257 p. http://dlib.rsl.ru/rsl01004000000/rsl01004888000/rsl01004888235/rsl01004888235.pdf
2. Oleg Glovatskii, Rustam Ergashev, Naira Nasirova, Jaloliddin Rashidov and Boybek Kholbutaev Experimental tests of submersible vane pumps E3S Web of Conferences 401, 05065 (2023) https://doi.org/10.1051/e3sconf/202340105065
3. Hou XB, Sun YQ, Song CP. Analysis on cam ring & vane arousing flow fluctuation for hydraulic vane pump. *Chinese Hydraul Pneum* 2008; 2008: 57–60.
4. Zhang QF, Yan PP, Shan JP. Numerical simulation of inlet and outlet pressures influencing internal flow of a vane pump. *ACTA Armamentarii* 2014; 35: 1223–1229.
5. Glovatskiy O.Ya., Nosirov F.Zh., Sharipov Sh.M., Saparov A.B. Study of the influence of cavitation on pressure pulsation behind the impeller of pumping units // Collection of scientific articles of the XV scientific and practical conference of young scientists and masters “Modern problems in agriculture and water management”, - Tashkent, 2016. - 425-430 p.